JOURNAL OF GEOPHYSICAL RESEARCH, VOL. 106, NO. E4, PAGES 7721–7732, APRIL 25, 2001

DIRTCam in the desert: The Silver Lake field test of the Robotic Arm Camera

R. Aileen Yingst,[1] Peter H. Smith, Mark T. Lemmon,[2] Robert L. Marcialis, James W. Rice Jr.,[3] and Jon D. Weinberg[4]

Lunar and Planetary Laboratory, University of Arizona, Tucson

Abstract. The Robotic Arm Camera (RAC) is a panchromatic imager included as part of the Mars Volatiles and Climate Surveyor (MVACS) science experiment on Mars Polar Lander and on the Mars 2001 lander. It is designed to take both panoramic and microscopic images in order to gather data on the morphology and mineralogy of surface materials. In order to demonstrate these capabilities, a field test was conducted at Silver Lake playa in the Mojave Desert. The test consisted of going to a remote site unknown to the science team and providing that team with a data set of RAC panoramic, anaglyph, and microscopic images similar to what would be available during an actual landing. With only this information the science team attempted a determination of the position and the geology of the field test site. Using panoramic and anaglyph images provided by RAC, in conjunction with overflight images simulating data from a descent camera, the landing site for the field test was determined within 50 m of the actual site as lying near both a playa and an alluvial fan. Images of samples from the surface and within the trench revealed grain morphology, texture, and mineralogy indicating a soil dominated by quartz and feldspar, interspersed with a minor mafic component. Grain-size distribution was bimodal, with small, rounded to subrounded grains dominant at lower depths and larger, more angular grains more plentiful near the surface. This mineralogy is confirmed by the geology of the site and the data provided by the descent images and mid-IR measurements. RAC has demonstrated its ability to image the local geology and identify the major mineralogic components of an unknown site. These abilities will be crucial in understanding both the macroscopic and the microscopic geology of future Mars landing sites. This test also has demonstrated the crucial link between RAC data and complementary data sets such as context images and compositional data that can support the mineralogic observations made by RAC.

1. Introduction

The Robotic Arm Camera (RAC) (aka DIRTCam, the Dust, Ice, Rock and Terrain Camera), designed to gather data on the morphology and mineralogy of surface materials, is a panchromatic imager with a focusable lens, mounted on the wrist of a robotic arm. RAC, shown in Figure 1 and Plate 1 (top), has heritage from the Mars Volatiles and Climate Surveyor (MVACS) experiment on Mars Polar Lander and has been included on the 2001 lander. In support of the digging mode for the robotic arm, RAC is designed to take in-trench images, which are enhanced to produce stereoscopic views by overlapping camera fields. After scraping up some surface materials on the scoop blade, the scoop can be moved to put the sample 11 mm in front of the window. The camera lens can then be focused to allow a microscopic image of the sample. A light-emitting diode (LED) array with three colors (red, green, and blue) illuminates the soil to allow true color imaging at a resolution of 23 microns per pixel. At far focus when the scoop is moved out of the way, the camera has a field of view (FOV) of 52° by 26°, making it useful as a panoramic camera; again, stereoscopic views can be created by overlapping fields [*Keller et al.*, 2000].

We conducted a field test outside of Baker, California, in the Mojave Desert in order to demonstrate several capabilities of the RAC imager. First, the camera obtained panoramic images of the test site to help a science team remotely located at Ames Research Center determine where to dig a trench. Second, anaglyphs of the "landing site," particularly the working area of the arm, were produced. Third, during the digging process (done by hand in the absence of working robotic arm) the camera was pointed to image the trench and tailings at 10-cm-depth increments. Fourth, color images at 25–50 μm/pixel resolution were obtained by illuminating soil samples taken at different levels in the trench with the colored lamps. In total, this data set mimics the type of data expected from Mars.

In addition to these instruments, the "lander" had a high-resolution stereo imager and a midinfrared spectrometer similar to the 2001 payload. In order to better simulate the 2001 APEX remote-sensing package, data were also available from Mini-TES [*Squyres et al.*, 1999], an instrument designed to

[1]Now at Department of Natural and Applied Sciences, University of Wisconsin–Green Bay, Green Bay, Wisconsin.
[2]Now at Department of Physics, Texas A&M University, College Station, Texas.
[3]Now at Department of Geological Sciences, Arizona State University, Tempe, Arizona.
[4]Now at Raytheon Electronic Systems, Tucson, Arizona.

Paper number 1999JE001190.
0148-0227/01/1999JE001190$09.00

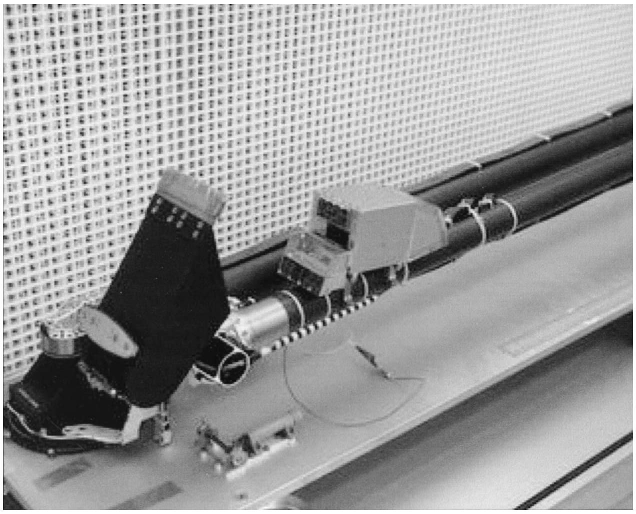

Figure 1. Robotic Arm with Mars Volatiles and Climate Surveyor (MVACS) camera attached.

return emission data from the thermal region of the spectrum. The scientists had access to the scene only through the data sets supplied by this instrument package and could send commands to the field crew to take data or dig deeper into the trench. In this manner the digging operation of the future mission was simulated.

2. Instrument Description

The Mars 2001 RAC is derived from MVACS [*Keller et al*., 2001], but the illumination system has been improved by replacing the incandescent colored lamps with LEDs. The camera development was a joint effort between the University of Arizona (UA) and the Max Planck Institute for Aeronomy (MPAe). The UA supplied optics, motors, and lamps, as well as the frame buffer board. The MPAe supplied the detector and its readout boards and integrated the camera head. After assembly in Germany the camera was tested and calibrated at the UA [*Keller et al*., 2001]. For the field test a prototype model was used; this prototype is referred to in this paper as DIRT-Cam.

The imaging area of the CCD is a 512 × 256 LORAL frame-transfer array with 23-μm pixels. A long-wavelength cutoff filter limits the spectral response to 450–700 nm. An $f/11.2$ double Gauss lens and focusing mechanism with stepper motor allows the camera to focus from 11 mm in front of the window to infinity with negligible aberration. An example of an in-scoop focus series for sand and soil is shown in Figure 2. The window has a motorized, protective sapphire cover. The cover will be lowered during digging operations and is clear so that failure in the down position is not fatal to operations. This cover glass is expected to become very dusty during the mission.

At the closest focus the image scale is ~1:1, so objects may be imaged at 23 μm/pixel. At the hyperfocal position, objects from 30 cm to infinity may be imaged at 1.85 mrad/pixel. Rather than interchangeable filters, RAC has red, green, and blue LEDs as an illumination system. Upper and lower LED assemblies illuminate the nearby surface or inside the scoop when it is retracted, and a third set of LEDs attached to the upper assembly illuminates the leading edge of the scoop in the near-focus position.

RAC is mounted near the wrist joint on the forearm of the Robotic Arm (RA), which is used to point the camera. The arm articulates in azimuth and elevation at the shoulder and in elevation only at the elbow. The arm also has an elevation-only wrist joint for scoop motion. The two arm sections are each 1 m long; RAC is mounted with the lens 28 cm from the wrist joint. The forearm of the 2001 RA is shorter than the MVACS RA. It has a grapple hook on the scoop joint, in lieu of the MVACS temperature probe, to allow the RA to be used as a crane to lift the rover Curie onto the surface of Mars.

3. Field Test Results

3.1. Field Test Goals

The RAC team set several goals for this field test. The first was to test the RAC's ability to acquire panoramic images when pointed by the RA. In principle, stereoscopic images could also be obtained, and this needed to be demonstrated. In addition to distant views with the RAC, close up images of the RA working area also needed to be examined so that we could understand what distance from the surface to take the images to maximize the quality of the final product. This would test RAC as a remote-sensing tool, where there is always the issue of coverage versus resolution.

The second goal was to understand how to use the RAC to support the digging process. A site with known subsurface layering was chosen to test the ability of the science team to find these layers during their analysis of the data sets. Questions to be answered here included what amount of overlap between images is needed to allow visualization of the trench and how to take images of the trench walls and bottom. We also attempted to illuminate the bottom of the trench with the LEDs once RAC was deep enough to be in dark shadow. RAC was used to image the tailings pile created by the soil removed from the trench.

Third, samples of surface material at each depth were examined in microscopic mode to learn how to evaluate soil types from the RAC-resolution images. For the purposes of this paper, the term "soil" is used in reference to any unconsoli-

Plate 1. (opposite) (top) MVACS DIRTCam mounted on the Robotic Arm. Visible in this image are (a) the entrance (CCD) window; the (b) upper and (c) lower lamp/filter rows, replaced by LEDs for Mars 2001; (d) the reflector plate; and (e) the temperature probe, which will be replaced by the rover grapple hook on Mars 2001. The scoop is designed to position itself in front of the entrance window for imaging of samples. The mounted lamps are placed so that at each focus the maximum illumination can be achieved inside the scoop. The upper lamps illuminate samples at close focus, while at far focus, the lower lamps are used. At intermediate focus, lamps mounted above the upper lamp row are activated and light is reflected off the reflecting plate and into the scoop. The sapphire protective window for the entrance window is mounted behind the reflecting plate and will rotate through an angle of 90° to a position exactly covering the entrance window. (middle) Anaglyph of a portion of the landing site near the trench area. The separation between images making up this anaglyph is 12 cm. (bottom) Anaglyph of trench walls at 10-cm depth. Note the structure visible in the trench layers as revealed by the stereo capability of DIRTCam.

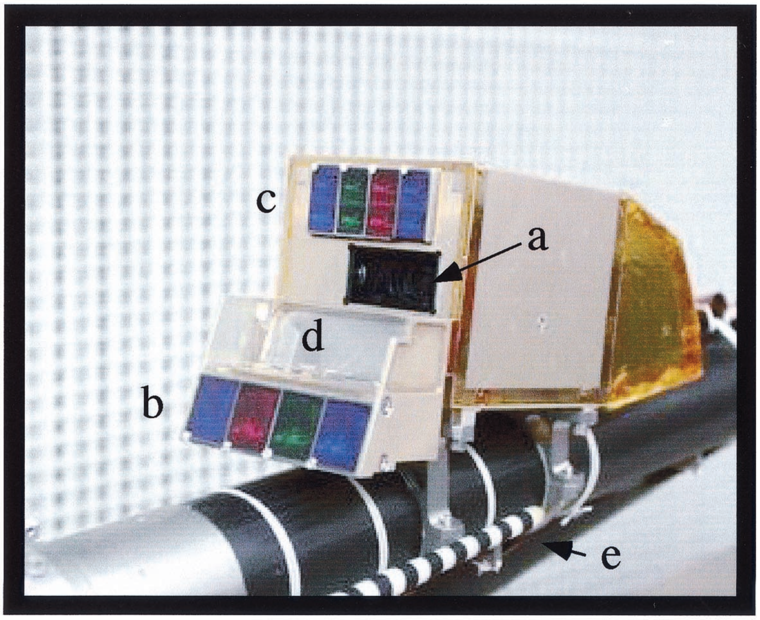
c
a
d
b
e

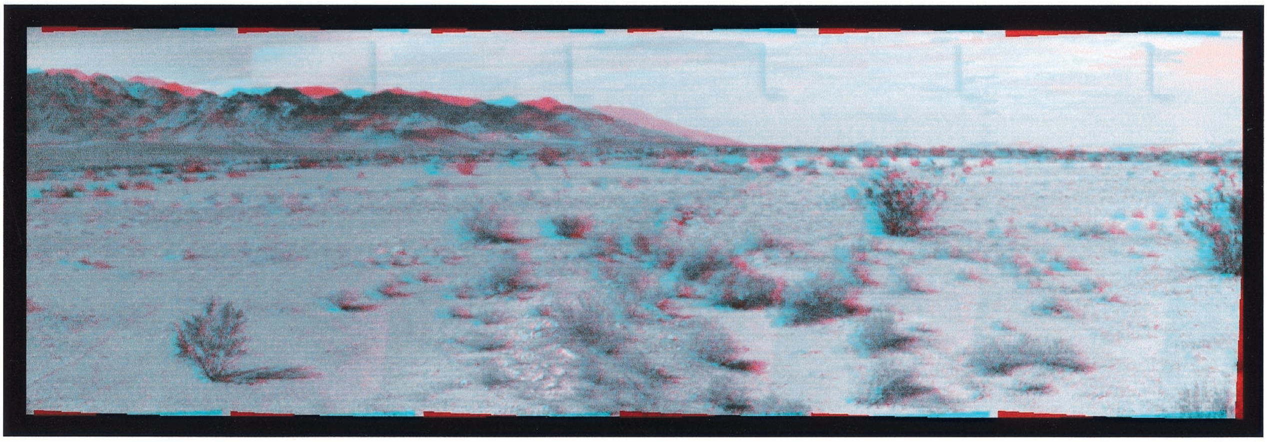

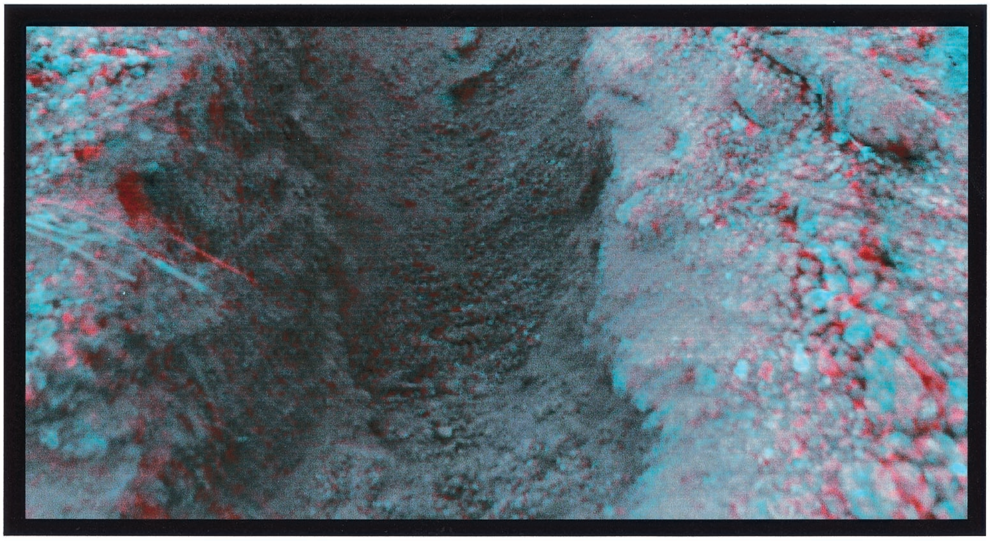

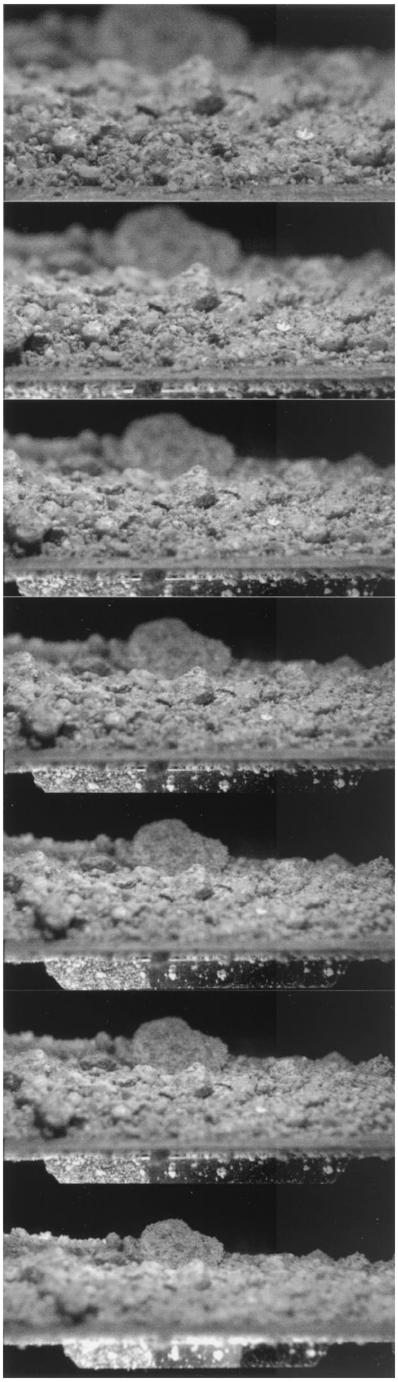

Figure 2. Focus series of witness sample extracted from 30-cm depth within the trench. This set shows (from top to bottom) 11-, 12-, 14-, 17-, 20-, 25-, and 31-mm focal stops. Note the variations in texture, shape, and grain morphology discernable at each focus. At far focus the angular morphology of the largest grains can be seen in detail, while at the closest focus the subtle morphology of sand-size grains can be discerned and grains <50 microns across can be resolved.

dated surface or subsurface (<50-cm depth) material of unknown composition. The goal was to determine the diversity of soil components, soil morphology, and the size distribution of the pebbles. Witness samples were also returned.

Finally, we wanted to test the ability of scientists to make the correct identifications of local geology using only the data from the RAC and the other available instruments. The team had the ability to send commands to the field team but could not ask any factual questions concerning the site. They were also unaware of the location of the site but were provided with unlabeled overflight images for context to mimic the data produced by the descent imager.

3.2. Field Test Setup

For the field test we used a prototype model of RAC (DIRT-Cam) with LEDs installed. We had no model of the arm to use, so we constructed a model of the forearm and mounted that to a telescope tripod. This arm had an elbow joint capable of azimuth and elevation motion and a wrist joint with a scoop attached. The scoop was an approximation of the Mars 2001 configuration with a set of abrasion patches added to the scoop bottom (part of the Mars Environmental Compatibility Assessment (MECA) experiment). The grappling hook for lifting the rover was not on the model.

Images were acquired in three modes. First, panoramic images were acquired by raising the elbow joint to ~2 m. In this configuration the shoulder joint was modeled as pointing vertically, so the azimuth rotation of the elbow in the model corresponds to a shoulder joint rotation. Images were acquired at three elevations: horizon and 15° and 30° below the horizon. These were mosaicked to create a full panorama. Second, trench images were acquired with the elbow joint <1 m off the ground. In this mode, trench panoramas were acquired either with elevation-only camera motion or with azimuth motion and a translation of the camera/RA assembly to simulate shoulder joint motion. Third, color images were acquired in the laboratory rather than the field test site. Color imaging was attempted in the field, but highly variable illumination from the partly cloudy sky and a strong wind that blew material out of the scoop prevented us from getting useful data.

3.3. Field Test Parameters

While the science team based itself at Ames, the DIRTCam field team deployed to a desert site outside of Baker, California, on February, 17–19, 1999. The camera was operated in a "stand-alone" mode via a portable generator, a Sun workstation, and the Bench Control Electronics (BCE). Our goal was to simulate flight science operations as much as possible, without the complexity of running an entire spacecraft. The team at Ames "commanded" the field team to perform sequences of tasks via telephone at sporadic intervals during operations. Resulting images were relayed to the team at Ames several times a day via satellite modem. The data analysis team was not informed of the exact location of the field operation.

On the first day of operations, two panoramas were obtained with DIRTCam. The first, shown in Figure 3 and Plate 1 (middle), was properly exposed for the surrounding terrain; the other was properly exposed for meteorological and horizon imaging. The intent of these pans was to allow the Ames team to train at locating the "landing site" from these images and aerial photography.

On the second day of operations, a mosaic of the simulated "arm workspace" was obtained and relayed to Ames. Using these images, "commands" were issued to identify the exact location to begin trench digging and where to pile the tailings. The field team manually dug a trench 50 cm deep, 1 m long, and 10–15 cm wide, displayed in Figure 4 and Plate 1 (bottom). For each 10 cm of progress, DIRTCam images were obtained of the trench and the tailings, and "witness samples," shown in

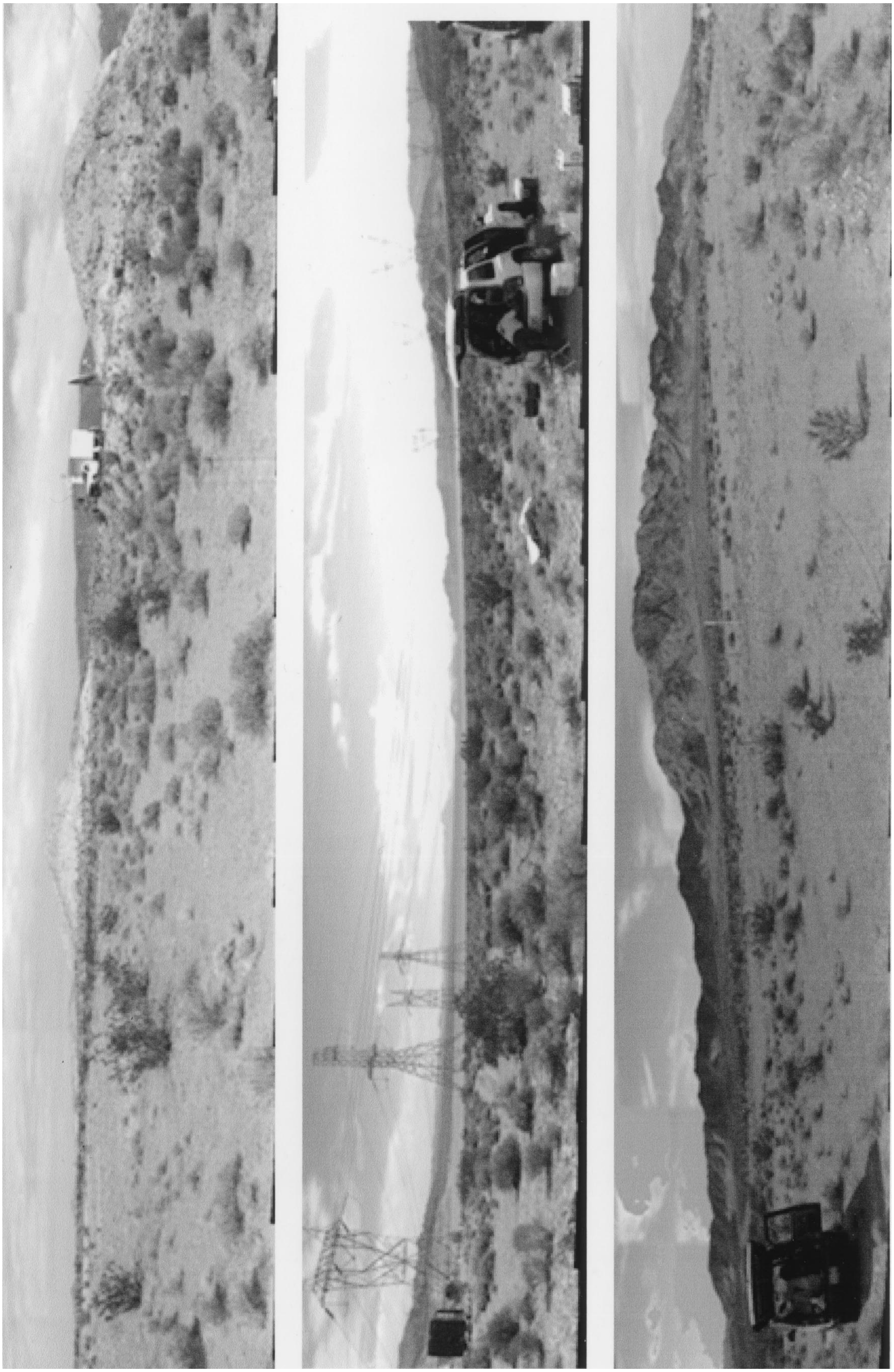

Figure 3. Panorama of the landing site.

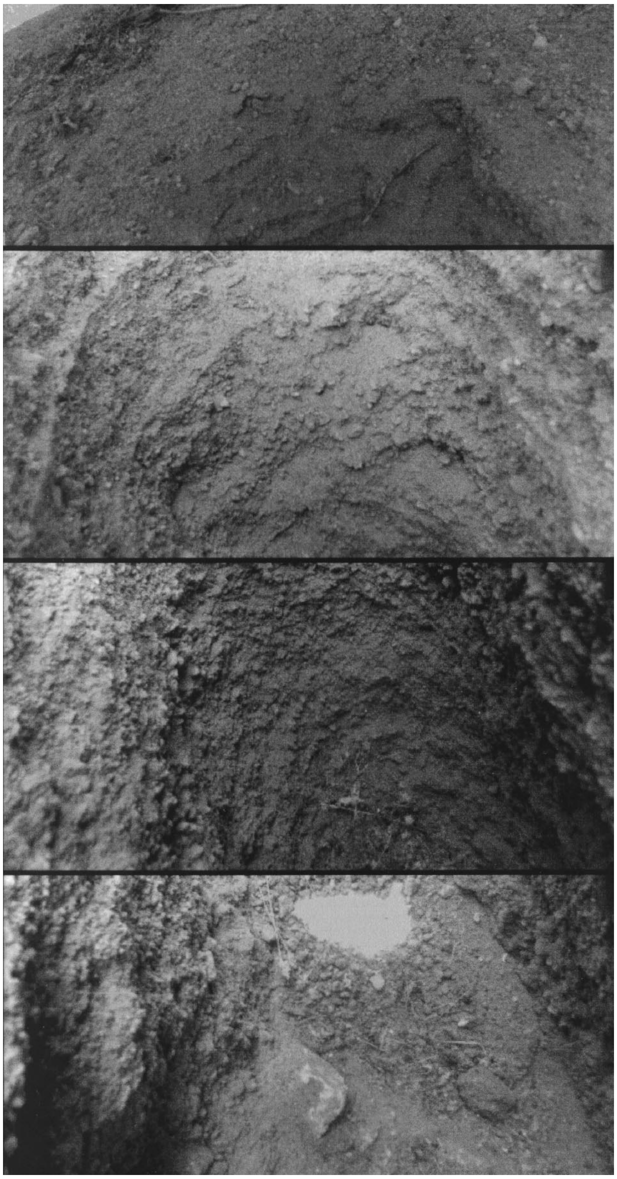

Figure 4. Mosaic image of trench walls at 50 cm depth, illuminated by ambient light, showing layering of the soil. A small pool of water sits at the bottom of the trench.

Figure 2, were collected for later analysis. Toward the end of digging operations the onboard lamps were used to provide color image sets of the trench bottom and walls. In-scoop imaging of soil retrieved from the trench was attempted several times, but, as mentioned above, the dryness of the soil, coupled with the high wind velocity, precluded attempts to get an RGB triad of the samples. These were taken later in the laboratory. Color imaging consisted of a background image illuminated by ambient light only and a set of three images, one with each color LED turned on. The background image was subtracted from each of the color images to give an RGB set. Images of a color calibration target allowed the creation of a single true color image from the set (e.g., Plate 2). Marsokhod (CCD) and Mini-TES images of the tailings were also obtained at 10-cm-depth intervals.

Cloud cover became increasingly variable and wind speed increased dramatically in the late afternoon of day 3 of the test. There is little doubt the thermal imaging was impacted by these conditions. However, the autoexpose algorithm was able to compensate for the variable illumination conditions.

The last phase of DIRTCam operations consisted of acquiring a sequence of images of the same scene, in the hope that changes due to saltation, or progressive forward movement of sediment particles through short, arcing hops, might be detected. Intermittent clouds complicated this process.

4. Field Test Results

4.1. Geologic Setting of the Test Site

The DIRTCam field test site is located on the shore of a dry playa called Silver Lake, lying northwest of the city of Baker, in the Mojave Desert, in central San Bernardino County, California, as shown in Figure 5. The DIRTCam field test was conducted at a different "landing site" than the previous Marsokhod rover tests. Silver Lake (26 km^2) is situated just east of the Soda Mountains (Precambrian metamorphics, including gneiss, schist, Mesozoic granitic intrusives, and dolostones) and north of Soda Lake playa (78 km^2), along the bottom of a wide, north-south running trough called the Silurian Valley. For a more detailed discussion of the regional geology and geomorphology, see *Grin et al*. [this issue] and *De Hon et al*., [this issue].

The elevation of the floor of Silver Lake is ~276 m, while the elevation of the floor of Soda Lake, located south of Silver Lake, varies from ~284 m in the south to ~281 m in the north [*Ore and Warren*, 1971]. These differences in playa floor elevations account for the fact that water must first fill Silver Lake to a depth of some 4.5 m before any water will accumulate in Soda Lake. Soda Lake is separated from Silver Lake by a low (3-m-high) topographic divide which formed by the merging of alluvial fans built out from the mountains on the east and west sides of the valley. A channel cuts across this divide and during times of flooding allows water to flow from Soda Lake into Silver Lake [*Thompson*, 1929]. The last occurrences of significant water levels in Silver Lake were a 3.0-m stand from January 1916 to July 1917 [*Thompson*, 1929], a 2.1-m stand from March 1938 to September 1939 [*Roger*, 1939; *Blaney*, 1957] and a 1.8-m stand in June 1969 [*Ore and Warren*, 1971].

Drainage into the Silurian Valley is and has been predominantly from the Mojave River basin, located to the southwest of the city of Baker. The Mojave River flows during times of heavy flooding, from its source region ~200 km to the southwest, to Silver Lake. During the late Pleistocene several pluvial lakes and spillways were formed along the course of the Mojave River. Outflow of one of these, Manix Lake, some 15,000 years ago [*Thompson*, 1929] formed a narrow, 8-km-long canyon (Afton Canyon) that drained the lake. The outflow spread out over a larger area and deposited its sediment load, forming a broad alluvial plain before flowing into the Silurian Valley. This overflow formed Lake Mojave (including the present day Soda and Silver Lakes [*Weldon*, 1982; *Ore and Warren*, 1971]), bounded on the west and southwest by the Soda Mountains and on the east by extensive pediments and alluvial fan surfaces from the Turquoise Mountains that slope gently in toward the basin. Lake Mojave consisted of two pluvial age lakes located in an elongate basin which now contains Soda Lake and Silver Lake playas [*Thompson*, 1929]. Lake Mojave filled and then spilled out to the north, where an outlet channel was carved and joined the waters of the Amargosa River. Finally, these waters drained into Death Valley and formed Lake Manly. Thus the Silver Lake region was considered as a Mars

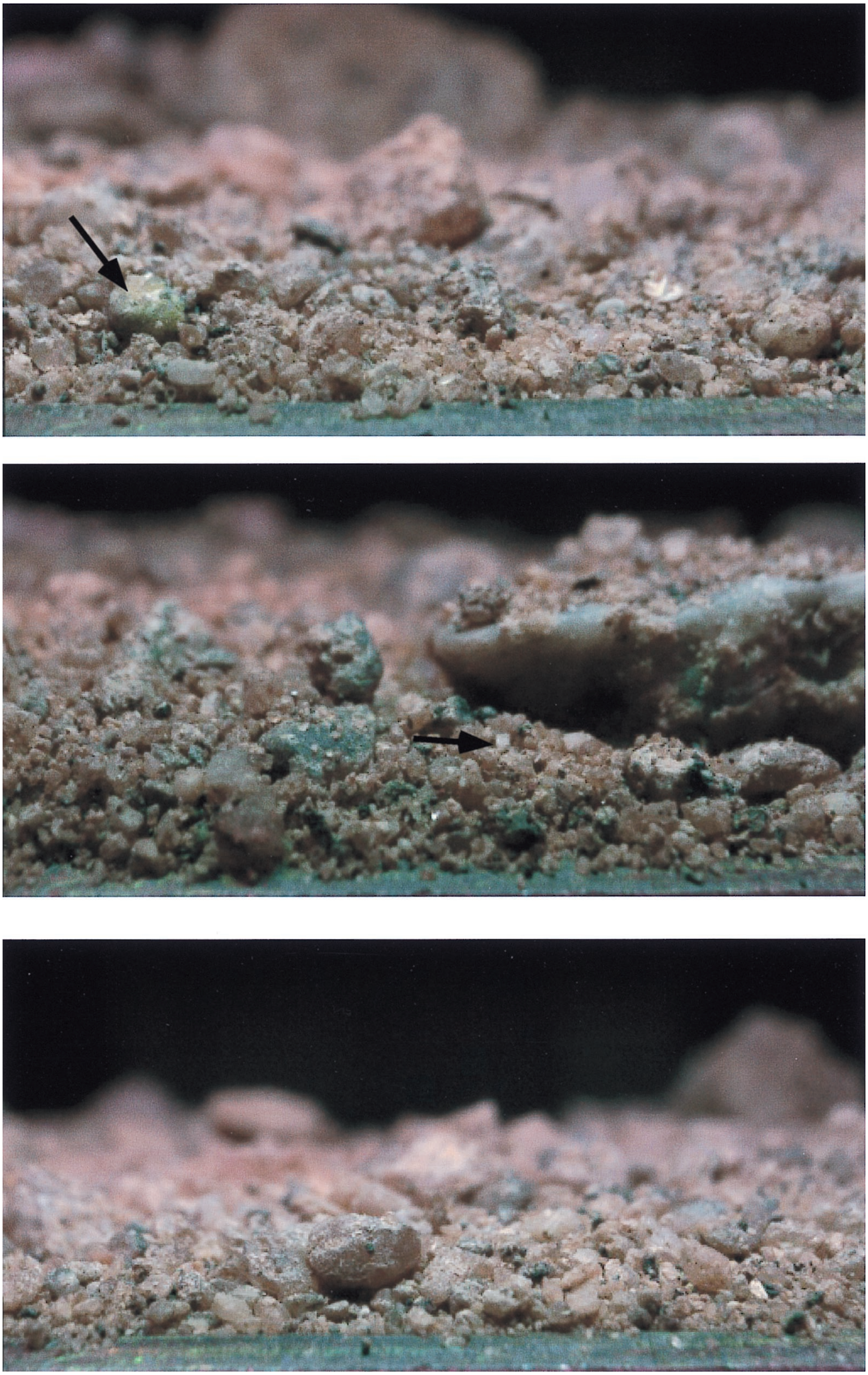

Plate 2. Color sequence of soils excavated from the trench at 30-, 40-, and 50-cm depth. Images are in focus at 10–11 mm and are ~11 mm across. The top image, taken of samples from 30-cm depth, shows clear, rounded to subrounded grains near the bottom of the image. These are likely quartz grains. The greenish feature indicated by the arrow at left is of organic origin. At 40-cm depth (middle image) a large conglomerate pebble can be seen, along with several angular, dark grains that are likely mafic. The squareness of the small white grain indicated by the arrow near the bottom of the image suggests the 90° cleavage planes of feldspar. The bottom image, taken of a sample from 50-cm depth, shows an abundance of small, rounded, clear grains, interspersed with larger pink grains. This likely represents a distribution of smaller, less resistant quartz and larger, more resistant feldspar soil components.

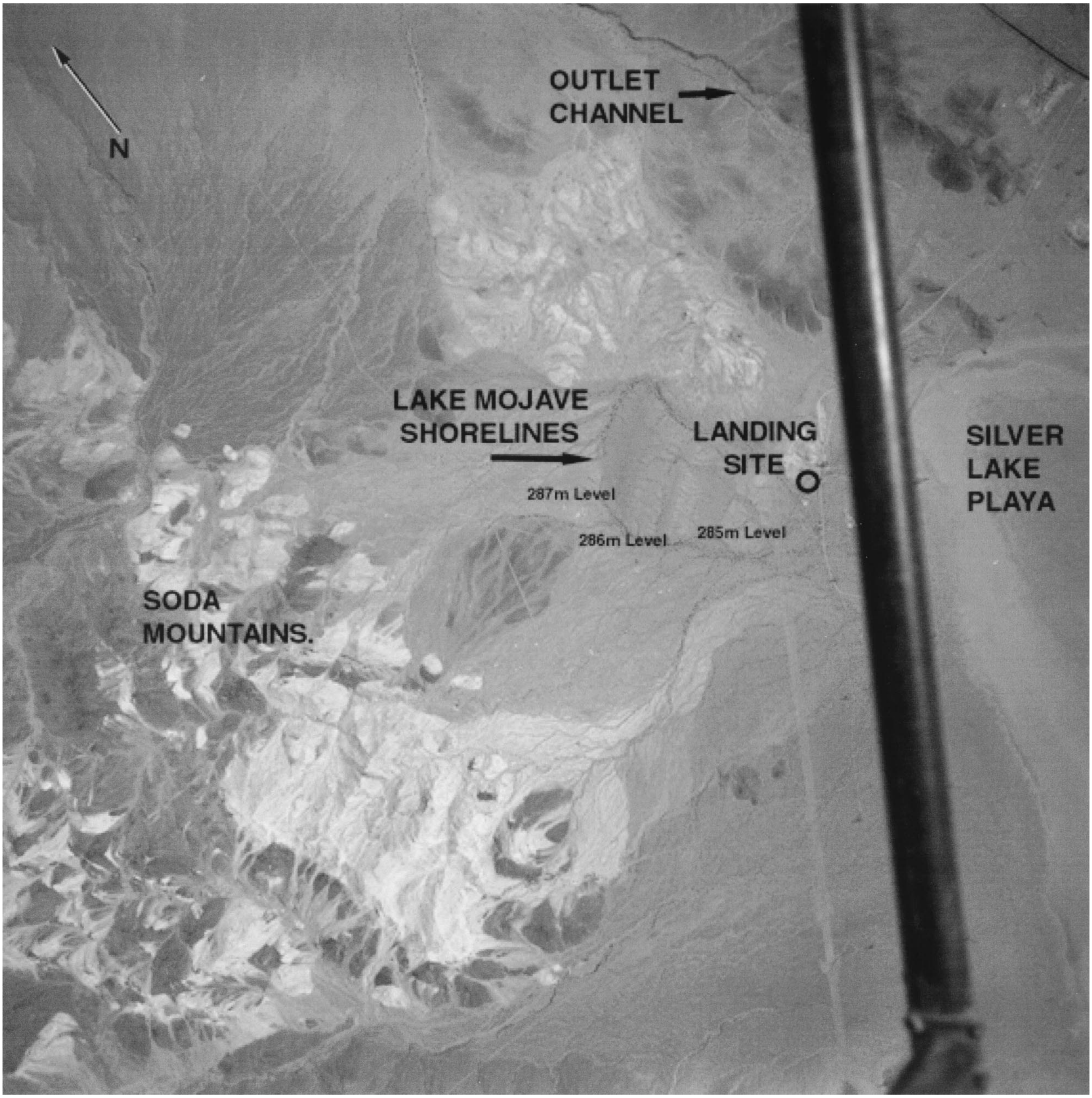

Figure 5. "Descent" image of field test site at 2.8 m/pixel showing the predicted and actual positions of the lander. Part of the helicopter structure cuts through the right portion of the image.

analog site in part because this scenario of cascading lakes and spillways may be a small-scale example of the formative processes of Martian paleolakes as proposed by *Scott et al*. [1991, 1992, 1995] and *Rice et al*. [1999].

Ore and Warren [1971] have constructed the following chronology for Lake Mojave on the basis of radiocarbon dates of shells and tufa. A major lacustral interval ended ~14,500 years ago with water overflowing the outlet channel, located at the northern margin of Silver Lake, at the 287-m level. The second lacustral interval lasted from 13,750 to 12,000 years ago and resulted in the development of extensive shoreline features at the same elevation. A less extensive shoreline is located at the 286-m level. The third high-water period, 11,000 to just over 9,000 years ago, resulted in the formation of shoreline features and the further downcutting of the outlet channel to the 285-m level. From 8,500 to 7,500 years ago a lake existed in the basin, but this lake did not overflow the outlet channel. A period of extensive drying began around 7,500 years ago. Surface rock alignments, abundant flakes, and artifacts suggest that early man was in the area 10,000 years ago [*Warren and DeCosta*, 1964].

The soil in this region is predominantly composed of subrounded to well-rounded quartz grains with some feldspar, mafic, and clay components. The subrounded to well-rounded grains are the result of fluvial transport through the Mojave River/lacustrine system with final deposition in a lacustrine environment (Lake Mojave). Wave action is responsible for the well-rounded grains, while larger clasts at the site were

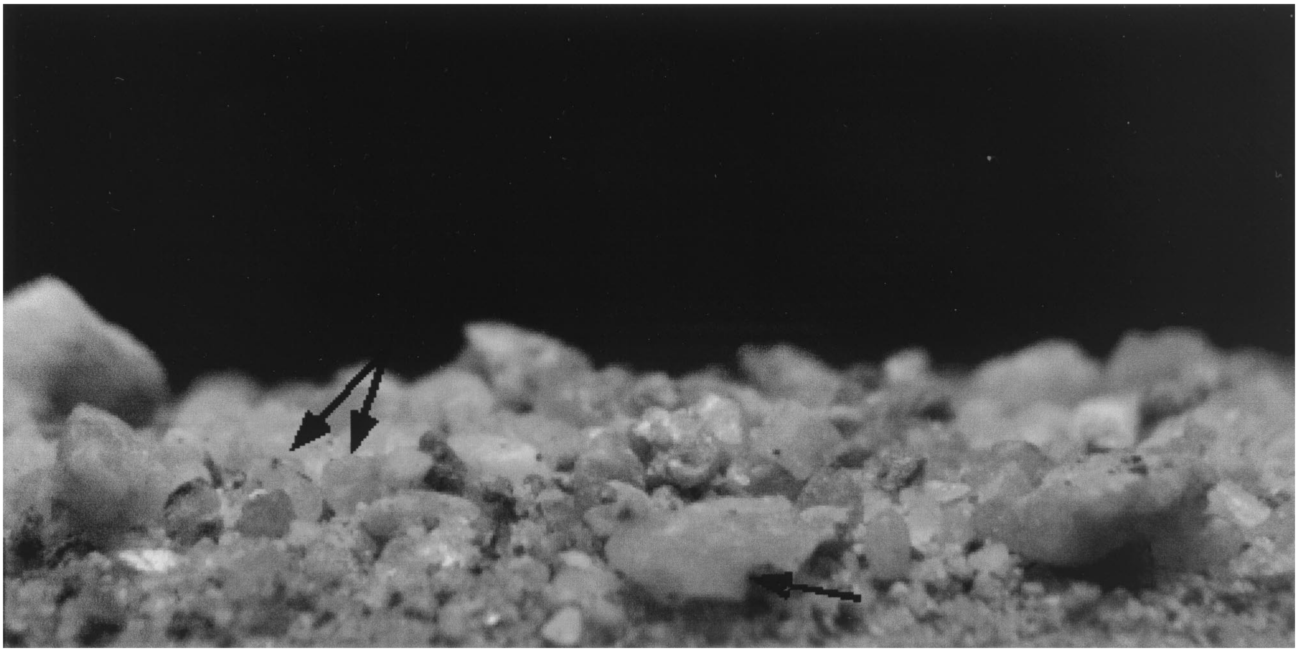

Figure 6. Fines (fine-grained soils) excavated from the trench at 50-cm depth. Image is in focus at 10–11 mm and is ~11 mm across. Here the roundness of the small grains typical of this trench level are seen in abundance. Fracture patterns suggesting quartz composition can be discerned in several grains near the bottom of the image.

brought down off the Soda Mountain alluvial fans by surface runoff and possibly debris flow processes.

4.2. Determination of Landing Site Location

Photogeologic analysis and remote-sensing analysis by the DIRTCam science team were conducted using orbital and surface imagery data sets. The orbital data set consisted of one orbital SPOT image (10 m/pixel), one "MOC class" image with a resolution of 2.8 m/pixel, comparable to images being returned by the Mars Orbiting Camera (MOC) on board Mars Global Surveyor, several Landsat Thematic Mapper images (30 m/pixel), and one airborne Thermal Infrared Mapping Spectrometer (TIMS) image [see *Stoker et al*., this issue, Figure 2]. The surface imagery data set was supplied by DIRTCam. The DIRTCam science team, unlike the Marsokhod rover science teams, did not have descent imagery at resolutions from 2.3 to 0.01 m/pixel.

The location of the landing site was accurately determined using the DIRTCam 360° panorama and MOC class image. This was accomplished by locating significant landmarks (mountain peaks, channels, playa surface, etc.) in both the panorama and the orbital image. The precise site was predicted to be as shown in Figure 5, situated on a local topographic high, some 10–15 cm above a nearby arroyo floor. On the basis of "orbital" and DIRTCam imagery it was concluded that the lander is located along an arroyo margin. The lower elevation region was interpreted to be the floor of a small channel that drains an alluvial fan. The predicted landing site is on the northwest margin of a playa situated below the lowest stand of three shorelines. This site is within ~50 m of the actual landing site, the same degree of uncertainty determined for the actual landing site. With the full sequence of descent images this accuracy could be improved even more.

4.3. Local Soil Analysis

Soil at the landing site consists of primarily fine-grained sand (0.0625- to 2-mm diameter) and gravel (granules, pebbles, and cobbles ranging from 2 to 64 mm in diameter) [*Wentworth*, 1922], with coarser-grained components intermixed. Figure 6 shows examples of these local soils, extracted from the trench at 30-, 40-, and 50-cm depths and magnified so that mineralogic and morphologic details of the individual grains may be seen. Close examination of soil samples taken at each 10-cm incremental layer of the trench reveals the general mineralogy and morphology of local soils and provides clues to the depositional history of the site, as detailed below.

4.3.1. Mineralogy. The fine-grained soil at all depths is dominated by a mixture of colorless and whiteish or pink minerals, as seen in Plate 2. The glassy luster is suggestive of quartz clasts, and the conchoidal fracturing of many of these grains is very diagnostic of quartz. In addition, the pearly luster and possible 90° cleavage of several white and light colored grains, as indicated in Plate 2, suggest feldspar grains. Finally, a number of dark grains exist, representing a possible mafic component.

Mini-TES spectral information concurs with this assessment from scoop images, indicating that the trench material is quartz-rich with some clay and no carbonates. Although the presence of carbonates was strongly suspected and searched for in all DIRTCam images, no grains displayed the rhomboidal cleavage that would be indicative of carbonates. This is a somewhat surprising result in light of the fact that TIMS imagery indicates that the mountains and some alluvial fans have carbonate composition. This may be explained by the fact that the channel that drains the local area begins in a quartz-rich region of low hills. However, this is puzzling since this same channel also cuts across the carbonate alluvial fan at the base

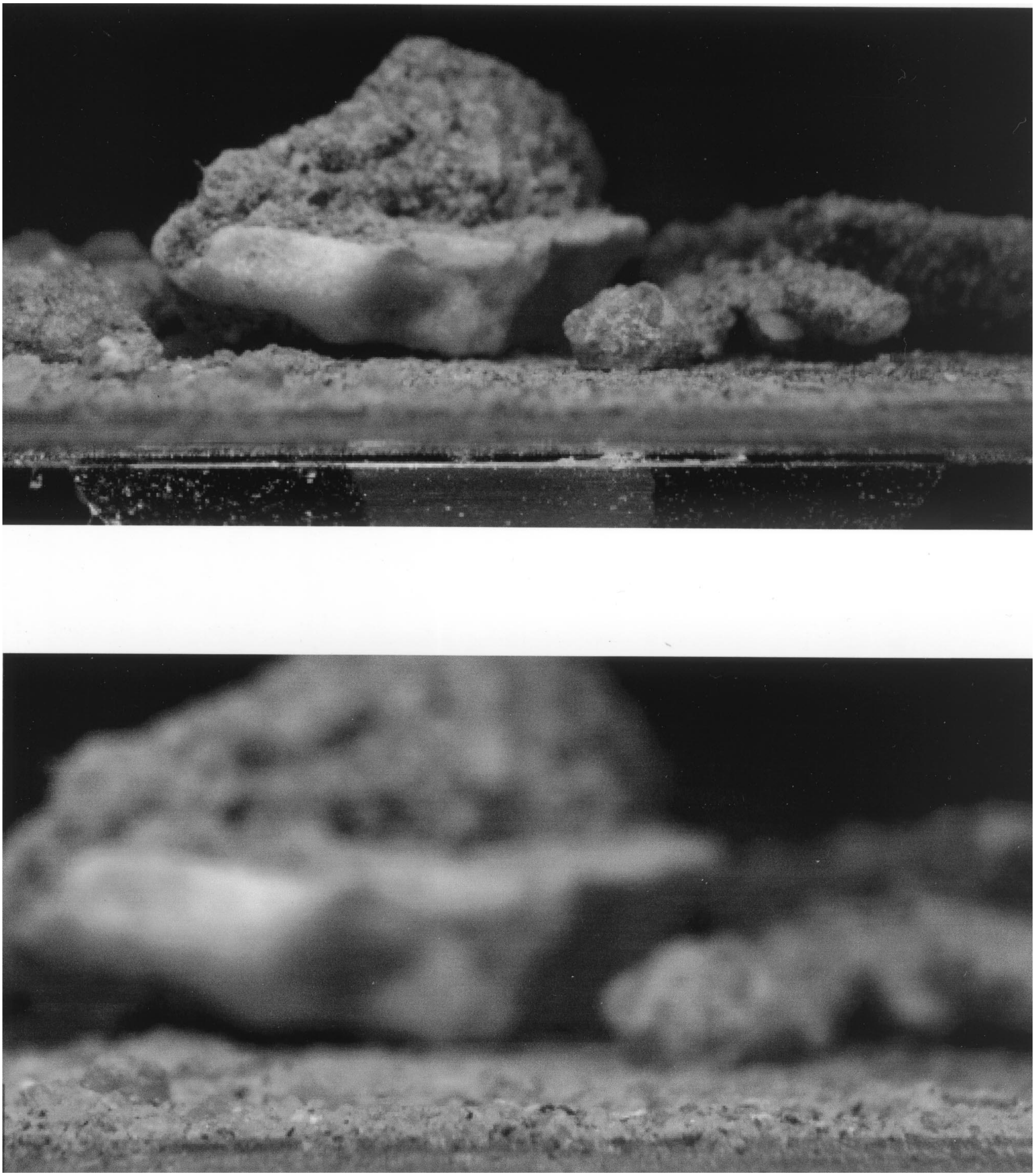

Figure 7. (top) Pebbles and (bottom) very fine soils excavated from the trench at 50-cm depth. The top image, in focus at 15–18 mm and ~20 mm across, shows the morphology of the larger conglomerate pebbles and the finer-grained matrix surrounding them. The bottom image, in focus at 10–11 mm and ~11 mm across, shows the very finest grains resolvable by DIRTCam. These grains are <30 microns across.

of mountains rich in carbonate and flows through the landing site area. We note that the lack of absolute mineralogical discriminators for carbonates due to the variability of carbonate species makes identification solely through DIRTCam images difficult.

4.3.2. Grain morphology. Two types of morphologies can be seen in the soil samples: a subangular coarse-grained component and a more rounded fine-grained unit. The coarser-grained material ranges in size from 3 to 7 cm in diameter. The finer-grained component of the regolith appears to range from fine to coarse sand-size particles (0.1–2.0 mm). These types, shown in Figures 6 and 7, are both found within the trench, surface, and tailings samples but are distributed differently in each sample set.

4.3.2.1. Grain shape: Although grain shape was not clearly visible in trench wall images, microscopic images of samples at different trench depths revealed a distribution of grain shape based on depth. At the deepest levels within the trench, approximately 30–50 cm deep, both pebbles and fines are very rounded but lack the frosted appearance that would suggest aeolian deposition. This likely indicates that fluvial deposition was dominant at this site. The proximity to a playa, on the basis of the identification of three extensive paleoshorelines in the MOC class image (2.8 m/pixel), is also strong evidence for fluvial rounding. Sand-size grains are thus interpreted to be rounded primarily by wave action in a lacustrine environment. Less rounded grains begin to appear at the 10-cm level, indicating that the most recent history of the site was no longer dominated by fluvial transport and deposition. The shapes of the largest gravel-size clasts are angular to subangular, indicating transport through fluvial runoff and possible debris flows for distances of several kilometers. These clasts were likely washed down from the Soda Mountains. There appears to be no correlation between mineralogy and grain size, so the resistance of these grains to various erosional processes cannot be determined from imaging these samples. However, the fine-grained, rounded morphology of the bulk of the local soil indicates continuous wave action in a lacustrine environment.

Surface pebbles are the most angular grains. Surface fines are rounded, although they do not appear to be as rounded as those found at deeper levels. These grains probably represent the most recent depositional layer and suggest emplacement by a combination of lacustrine fluvial activity and runoff from the local massifs. Larger, more heterogeneous grains comprise a minor percentage of samples at all levels. They occur frequently at the shallower trench layers, decreasing in frequency with depth, and are most common at the surface. These large grains appear to be mixed pebbles composed of large, angular grains of mineralogy similar to the surrounding soils, embedded in a fine-grained matrix. Mixed pebbles are most likely conglomerates of local detritus in a hydrous-mineral matrix, an observation supported by the Mini-TES measurements, which indicate a clay component in the soils. The saltation experiment conducted on the final day of the field test showed minimal motion of sand-sized surface grains; precisely one grain moved during the course of the experiment. This suggests that the surface at the landing site has developed a resistant layer, a common feature in desert environments, where salts dissolved in rainwater are left behind after evaporation and bind to form a duricrust. The majority of the surface soil is thus interpreted to be composed of resistant quartz and feldspar, interspersed with less rounded, presumably more recently deposited grains of similar composition at shallower levels and ultimately capped by a duricrust.

4.3.2.2. Sorting: The trench wall material and tailings pile both appear to have a bimodal size distribution: coarse and fine sand grains with pebbles interspersed throughout. There was no evidence for a mature, well-developed lag deposit, such as a desert pavement. Specifically, no coarse grain-to-grain contact was observed on the surface at the trench site, and fines were present in every level, while formation of desert pavement requires the winnowing out of surface fines over time [*McFadden et al.*, 1987]. It likely represents intermittent high-energy fluvial deposition from the alluvial fan. The trench layering could be easily seen, even in the portion of the trench in shadow, owing to successful illumination of the trench bottom by DIRTCam's LEDs. This layering consisted of irregular, discontinuous layers of coarse-grained material and fines alternating with finer-grained layers near the surface, with the coarse-grained layers appearing much less frequently with depth. Poor sorting of grains argues against a predominantly aeolian deposition history. The tailings pile and trench morphology thus demonstrate the bulk distribution of soil materials, with the more recently deposited, coarser, angular grains found near the surface coming from reworking of the alluvial fan through recent runoff and the deeper, highly rounded finer grains laid down as lakeshore deposits.

4.3.3. Site truthing. Types of grains identifiable by DIRTCam include quartz sand, feldspars, dark, possibly mafic material, and conglomerate pebbles (presumably sand or other larger material in a mud/clay matrix). This diverse mineralogy is consistent with one derived from the alluvial fan and playa environments described by *Thompson* [1929] and *Ore and Warren* [1971]. The general roundness of deep-level soil grains suggests that much of the soil from the test site is composed of durable quartz and feldspar grains that have been fluvially deposited, with minor components of mafic and other detritus emplaced through runoff from the surrounding massifs. These observations are also consistent with the contextual geology shown in the descent images and interpreted in previous studies [e.g., *Thompson*, 1929; *Ore and Warren*, 1971]. In addition, we have noted the change in dominant depositional mechanisms at the site, as suggested by the sorting of soil layers, and their gradation in shape from more to less rounded. However, no evidence in grain morphology, mineralogy, or sorting was seen for the early lacustral history of the landing site, as described by *Ore and Warren* [1971]. This is most likely due to the relatively shallow depth of the excavated trench, which likely penetrates only to layers <12,000 years old. Finally, the most surprising scientific result is the lack of carbonates observed in the samples, despite the proximity of the test site to a carbonate-rich playa. This observation by DIRTCam is nevertheless confirmed by Mini-TES and TIMS data retrieved from the site.

5. Discussion and Applications for Mars

5.1. Summary of Scientific Results

Types of grains identifiable by DIRTCam in this region include quartz sand or quartz clasts, feldspars, and clay-rich conglomerate pebbles (presumably sand or other larger material in a mud-clay matrix). This mineralogic diversity is expected from the geology of the site, a region with a high amount of vertical transport from local massifs to the low-lying alluvial fan. This result is also consistent with both the data provided by the descent images and the mid-IR TIMS measurements. The lack of carbonates observed in the samples is confirmed by data at mid-IR wavelengths, despite the proximity of the test site to a carbonate-rich playa.

5.2. Lessons Learned and Mars Applications

The panoramic and microscopic imaging capabilities of DIRTCam allowed us to identify the diverse mineralogy of the test site. Although we did not have available medium resolution images that would allow us to discriminate between general rock types, the major components that constitute rocks typical of the site were clearly discerned and noted. In conjunction with descent images, the field team was also able to use DIRTCam images to deduce the general geologic history of the site through analysis of grain mineralogy and sorting.

However, since many minerals, such as carbonate, have few or no discriminators in terms of mineralogic characteristics, DIRTCam images cannot reveal soil components with absolute accuracy. For instance, the field team would not have been able to confirm the absence of carbonates in the DIRTCam images without supporting evidence from the local (Mini-TES) and contextual (TIMS) thermal data. This example demonstrates that all data sets must be utilized concurrently; communication between instrument teams is crucial. Also, DIRTCam will necessarily be limited to exploring the most recent history of the Mars landing site since the trench dug by the RA will be shallow. Although Mars may not have as active a deposition system as Earth, it must be remembered that analysis of the landing site will likely be limited to the youngest geologic layers.

In this field test the DIRTCam prototype for the RAC has demonstrated its ability to panoramically image the local geology and identify the major mineralogic components of an unknown site. These abilities will be crucial in understanding both the macroscopic and the microscopic geology of the Mars Polar Lander and Mars 2001 landing sites.

Acknowledgments. We wish to acknowledge the technological assistance of MPAe in the design and setup of DIRTCam. We also gratefully acknowledge the time, effort, and funding of NASA Ames that made this field test possible.

References

Blaney, H. F., Evaporation study at Silver Lake in the Mohave Desert, California, *Eos Trans. AGU*, *38*, 209–215, 1957.

De Hon, R., N. G. Barlow, M. K. Reagan, E. A. Bettis, C. T. Foster, V. C. Gulick, L. S. Crumpler, J. C. Aubele, M. G. Chapman, and K. L. Tanaka, Observation of the geology and geomorphology of the 1999 Marsokhod test site, *J. Geophys. Res*., this issue.

Grin, E. A., M. K. Reagan, N. A. Cabrol, E. A. Bettis, C. T. Foster, C. R. Stoker, T. L. Roush, and J. E. Moersch, Geological analysis of the Silver Lake Marsokhod field test from ground-truth sampling and mapping, *J. Geophys. Res*., this issue.

Keller, H. U., et al., The MVACS Robotic Arm Camera, *J. Geophys. Res*., in press, 2001.

McFadden, L. D., S. G. Wells, and M. J. Jercinovich, Influences of eolian and pdogenic processes on the origin and evolution of desert pavement, *Geology*, *15*, 504–508, 1987.

Ore, H. T., and C. N. Warren, Late Pleistocene-early Holocene geomorphic history of Lake Mojave, California, *Geol. Soc. Am. Bull*., *82*, 2553–2562, 1971.

Rice, J. W., Jr., V. R. Baker, and D. H. Scott, Cascading lakes, spillways, and subaqueous debris flows: Models for Martian paleolakes, in *The Fifth International Conference on Mars*, p. 6241, Lunar and Planet. Inst., Houston, Tex., 1999.

Rogers, M. J., Early lithic industries of the lower basin of the Colorado River and adjacent desert areas, *San Diego Mus. Pap*. *3*, San Diego, Calif., 1939.

Scott, D. H., J. W. Rice Jr., and J. M. Dohm, Martian paleolakes and waterways: Exobiologic implications, origin of life and evolution of the biosphere, *Origin Life Evol. Biosphere*, *21*, 189–198, 1991.

Scott, D. H., M. G. Chapman, J. W. Rice Jr., and J. M. Dohm, New evidence of lacustrine basins on Mars: Amazonis and Utopia Planitiae, *Proc. Lunar Planet. Sci. Conf., 22nd*, 53–62, 1992.

Scott, D. H., J. M. Dohm, and J. W. Rice Jr., Map showing channels and possible paleolake basins, *U.S. Geol. Surv. Misc. Invest. Ser., Map I-2461*, 1995.

Squyres, S. W., et al., The Mars 2001 Athena Precursor Experiment (APEX), *Lunar Planet. Sci. Conf., 30th*, 1672, 1999.

Stoker, C. R., et al., The 1999 Marsokhod rover mission simulation at Silver Lake, California: Mission overview, data sets, and summary of events, *J. Geophys. Res*., this issue.

Thompson, D. G., The Mojave Desert region, California: a geographic, geologic, and hydrologic reconnaissance, *U.S. Geol. Surv. Water Supply Pap*., *578*, 759 pp. 1929.

Warren, C. N., and J. DeCosta, Dating Lake Mohave artifacts and beaches, *Am. Antiquity*, *30*, 206–209, 1964.

Weldon, R. J., II, Pleistocene drainage and displaced shorelines around Lake Manix, in *Geologic Excursions in the California Desert*, edited by J. D. Cooper, pp. 77–81, Geol. Soc. of Am., Boulder, Colo., 1982.

Wentworth, C. K., A scale of grade and class terms for clastic sediments, *J. Geol*., *30*, 377–392, 1922.

M. T. Lemmon, Department of Physics, Texas A&M University, College Station, TX 77843-4242. (lemmon@physics.tamu.edu)

R. L. Marcialis and P. H. Smith, Lunar and Planetary Laboratory, University of Arizona, P.O. Box 210092, Tucson, AZ 85721.

J. W. Rice Jr., Department of Geophysical Sciences, Arizona State University, Tempe, AZ 85287-1404. (jrice@asu.edu)

J. D. Weinberg, Raytheon Electronic Systems, P.O. Box 11337, Building 810, M/S 4, Tucson, AZ 85734.

R. A. Yingst, Department of Natural and Applied Sciences, University of Wisconsin–Green Bay, Green Bay, WI 54311. (yingsta@uwgb.edu)

(Received September 28, 1999; revised January 12, 2000; accepted February 2, 2000.)